RESEARCH PAPER

The Effect of Niobium Addition on the Microstructure and Tensile Properties of Iron-Nickel Base A286 Superalloy

Reza Soleimani Gilakjani[1], Seyed Hossein Razavi[1*] and Masoumeh Seifollahi[2]

** hrazavi@iust.ac.ir*

Received: April 2020 Revised: August 2020 Accepted: September 2020

[1] School of Metallurgy and Materials Engineering, Iran University of Science and Technology, Narmak, Tehran, Iran

[2] Metallic Materials Research Center (MMRC), Malek Ashtar University of Technology, Tehran, Iran

DOI: 10.22068/ijmse.18.1.7

Abstract: *Niobium is a significant addition to superalloys to enhance high-temperature mechanical properties. The purpose of this study is twofold: (1) to investigate the η and γ/ phase precipitations along with (2) to identify the high-temperature tensile properties in A286 and Nb-A286, as a modified type. The heat treatment of both alloys was carried out in a two-stage aging procedure at 760 °C for 16 h and 820 °C for 2 to 30 hours, then characterized by optical and scanning electron (SEM-EDS) microscopies, differential thermal analysis (DTA), and high-temperature tensile tests. The results showed that niobium addition increased the volume fraction of γ/ phase, from 10.7 % to 12 %, decreased its size, from 94 to 71 nm, and intensified the γ/-dissolution temperature from 987 °C to 1007 °C. Moreover, the γ/ to η phase transformation was sluggishly occurred in Nb-A286 due to the higher stability of γ/ precipitations. Furthermore, the Nb-A286 alloy demonstrates higher mechanical properties than the A286 one, approximately 100 MPa improvement, which was contributed to the much larger volume fraction and finer size of more stabilized γ/ phase.*

Keywords: *A286 superalloy, Niobium addition, η and γ/ phases, Microstructure evaluation, Hot-tensile properties.*

1. INTRODUCTION

A286 superalloy, as the most common iron base superalloy, can be used in hot sections of gas turbine engines, because of its mechanical properties and phase stability at high temperatures [1, 2]. This superalloy with high strength and corrosion resistance at moderate temperatures is widely used in the manufacturing of land-based, marine, and air gas turbines [3]. According to some studies, the formation of the η phase during solidification, heat treatment, and operation reduces the volume fraction of strengthening phases such as γ' phase. Therefore, the formation of such phases can lead to a decrease in mechanical properties [4, 5]. Also, according to some other studies, the precipitation of the η phase at the grain boundary not only does not cause the embrittlement of the nickel-base superalloys at high temperatures but can act as a barrier against boundary slip by precipitation at the grain boundary [6].

After exposure to a temperature of about 730 °C for a short time, this alloy becomes unstable and thus its γ' strengthening phase is transformed into a topologically closed packed (TCP) η phase with cellular or Widmanstatten morphology at or within the grain boundary [7, 8]. Seifollahi et al. [9] showed that the η phase did not form in the temperature range of 650 to 720 °C, precipitated at higher temperatures in the range of 780 to 850 °C that its amount increased with temperature and time.

Various studies on optimizing heat treatment cycles, adding alloying elements to the chemical composition, and so on have been conducted to control the η phase [10].

Studies on the effect of niobium on iron-nickel-base superalloys show that the addition of this element, by dissolving into the austenitic matrix of superalloy, increases the strength through the solid solution mechanism. On the other hand, the increase of γ' volume fraction enhanced the alloy stability, and consequently, improves the strength, fatigue life, and creep resistance of the superalloys [11-14]. Rho et al. [15-17] showed that the addition of niobium to the A286 superalloy improved the fatigue life and creep resistance of the alloy by delaying the formation of the η phase.

So far, extensive research has been done into investigating the precipitation mechanisms of the η phase and the effect of this phase on the mechanical properties of iron-nickel base superalloys [3, 18-20]. However, few studies have been conducted on the effect of niobium addition

[DOI: 10.22068/ijmse.18.1.7]

on the rate, morphology, and precipitation mechanisms of the η phase and its effect on the tensile properties of the A286 superalloy. Besides, sometimes conflicting results have been reported. This study aims to add niobium to the chemical composition of the A286 superalloy and investigate the effect of its presence on the η phase formation and mechanical properties of this alloy.

2. MATERIALS AND METHODS

The A286 and Nb-modified A286 superalloys were melted and poured in a vacuum induction melting (VIM) furnace at the pressure of 10-3 Pa. The chemical composition of cast ingots was determined by the spectroscopy method. Table 1 shows the chemical compositions of the two alloys investigated. Homogenization treatment of as-cast ingots was performed at 1180 °C for 6 hours and air cooled. The homogenized samples were subjected to a hot rolling process at 1100 °C up to 50 % reduction. The wrought alloys solutionized at 980 °C for one hour subsequently cooled in water.

The 5 × 5 × 5 mm^3 specimens were subjected to aging heat treatment in the temperature range of 650 to 900 °C for 2 to 30 h to evaluate the η phase. An electrical resistance furnace with a temperature accuracy of ±5 °C was used for heat treatment. The specimens were etched with a glycerol solution after polishing. The Nikon Epiphot 300 optical microscope and Philips XL40 scanning electron microscopy (SEM) which is equipped with energy-dispersive X-ray spectroscopy (EDS) at a voltage of 30 kV were used to study the microstructure and distribution of phases. Quantitative analysis of metallographic images was performed by Clemex software. DSC[1] Mettler Toledo optical emission spectrometer was used to determine the transformation temperatures of the η and γ' phases with heating and cooling rates of 10 °C/min. The temperature range of heating and cooling of the samples was selected between 350 and 1400 °C. The tensile properties of both alloys were measured at 650 °C using a computer-connected Instron Model 8502 testing machine. Then, JMatPro 7.0 software was used to simulate the thermodynamic diagrams. This software is based on the calculation of phase diagram (CALPHAD) which mathematically analyses the thermodynamic of the system. Using the thermodynamic properties of phases, phase equilibrium is calculated by a Gibbs energy minimization process [21].

3. RESULTS AND DISCUSSION

3.1. Microstructural Studies

Fig.1 shows an SEM BSE[2] mode image of A286 and Nb-A286 microstructure after aging heat treatment at 720 °C for 16 h. The study of the microstructures of both superalloys (Fig. 1) by Clemex software shows that there is an increase in the volume fraction of the γ' strengthening phase from 10.7 to 12 volume percent and a decrease in the average size of this phase from 94 nm to 71 nm, due to the addition of niobium. Adding niobium to the chemical composition of iron-nickel base superalloys leads to the occupation of the interstitial spaces of the matrix austenite phase by niobium atoms. Also, by adding niobium, a decrease in the solubility limit, and an increase in the activity of Al and Ti elements in the matrix phase are observed. As a result, the nucleation sites and the volume fraction of the γ' phase are increased [22]. The dissolution of the niobium element in the γ' phase increases the stacking fault energy and delays the transformation of γ' to η phase [23, 24]. The presence of niobium in the matrix also reduces the diffusion rate in the matrix, and consequently, decreases the growth rate of γ' phase and its size [22].

To evaluate the η phase precipitation, a two-stage aging treatment was performed on samples. Fig. 2 shows optical microscope images of A286 and Nb-A286 microstructures after two-stage aging heat treatment at 720 °C for 16 h and then at 820 °C for 8 h. Fig. 2 shows the twins, austenitic matrix, and η phases. As shown in Fig. 2, at similar aging times and temperatures, Nb-A286 superalloy had a lower η phase volume fraction than the A286. Clemex software analysis showed that the η phase volume fractions for A286 and Nb-A286 superalloys were 3.5% and 1%, respectively. Fig. 2 shows that the addition of niobium has prevented the precipitation of the Widmanstatten η phase. For η phase, two types of cellular (for lower times and temperatures) and Widmanstatten morphology (for higher times and temperatures) are observed [25, 26].

[1] Differential Scanning Calorimetery

[2] Back Scattered Electron

[DOI: 10.22068/ijmse.18.1.7]

Table 1. Chemical composition of A286 and Nb-A286 superalloys (wt%).

Alloy \ Elements	Fe	Ni	Cr	Al	Ti	Nb	Mo	Mn	Si	V	C	B
A286	Bal.	25.3	15	0.45	2.25	---	1.35	0.93	0.21	0.3	0.04	**0.006**
Nb-A286	Bal.	24.8	14.7	0.42	2.22	0.52	1.38	1	0.26	0.23	0.03	**0.005**

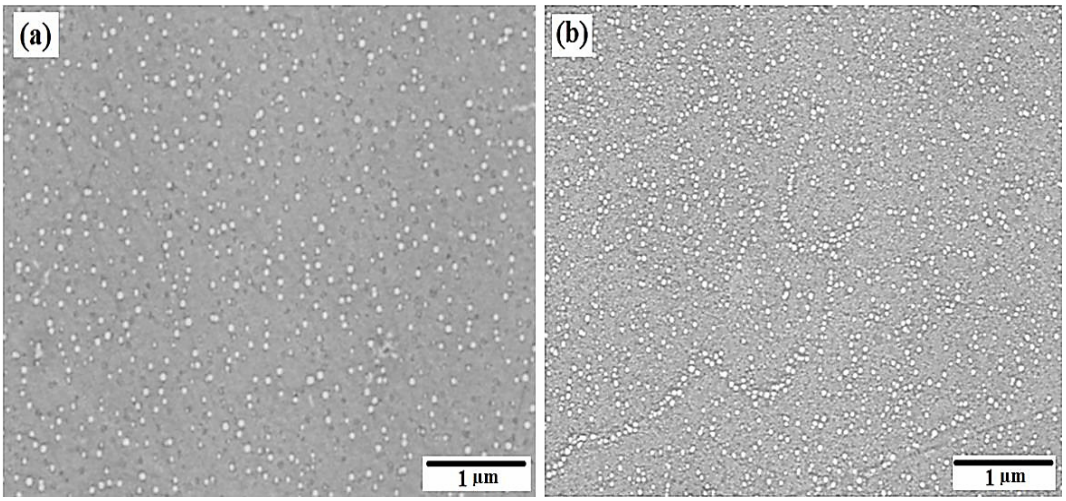

Fig. 1. SEM BSE mode image of γ' precipitations after aging heat treatment at 720 °C for 16 h (a) A286 and (b) Nb-A286.

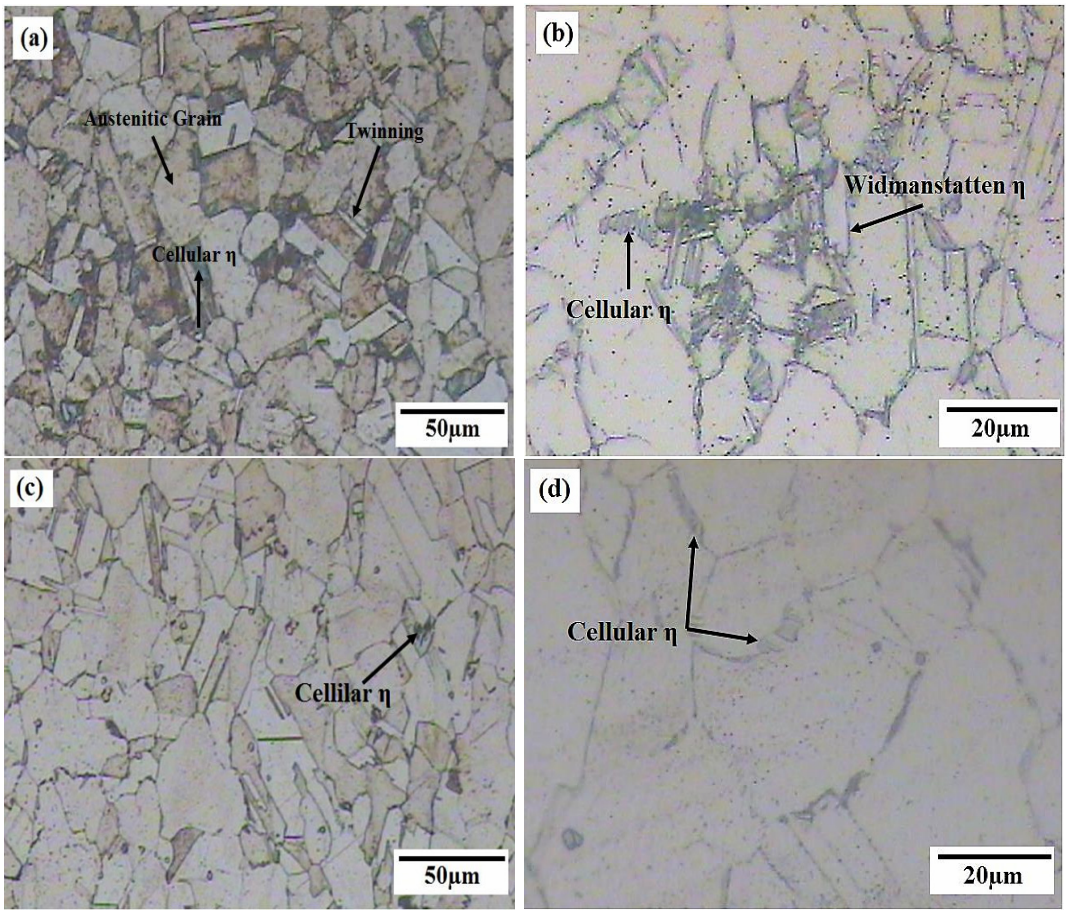

Fig. 2. The microstructure after aging heat treatment at 820 °C for 8 h (a, b) A286 and (c, d) Nb-A286.

[DOI: 10.22068/ijmse.18.1.7]

Titanium must diffuse through the grain to form the η phase by increasing the nickel/titanium ratio to 3. With the dissolution of niobium in the matrix phase, the titanium diffusion, and consequently, the formation of the η phase becomes more difficult [20]. The occupancy of the titanium diffusion path by niobium is one of the reasons for decreasing the volume fraction of η phase and increasing its formation temperature. In addition to this mechanism, since niobium tends to be present in the γ' phase, it enters to γ' lattice and increases its stability.

Many studies have been conducted on the role of Nb, Al, and Ti in the formation of γ' in Fe-Ni-based superalloys, which reveal quite equal participation of these elements [27-30]. Table 2 lists the EDS analysis of γ' and η phases.

Considering the heat treatment and metallographic evaluation of each sample, TTP curves of start and precipitation of η in annealed for both alloys are shown in (figure 3). Precipitation of η phase depends on the diffusion rate of Nb and Ti and the activation energy of phase transformation (Ti quantity and supersaturation of solution). THE C-shaped TTP curve is due to the interaction of these two parameters. Increasing the weight percent of Nb shifts the curve to the right and delays the equilibrium transformation of η phase. In other words, the formation of η phase occurs in a narrow range of temperature and time. Also, the peak temperature of η phase formation increases from 840 °C to 860 °C. Thus, increasing the Nb in the alloy will result in the formation of η phase at higher temperatures and longer times.

Table 2. Results of DTA test a) A286 and b) Nb-A286.

Point Number	1 (°C)	2 (°C)	3 (°C)	4 (°C)	5 (°C)	6 (°C)	7 (°C)
Point Situation	T_f GP Zone	T_f γ'	T_f η	T_sγ'	T_sη	T_sMC	T_m
A286	420	705	823	982	1100	1331	1406
Nb-A286	424	687	839	1007	1136	1327	1398

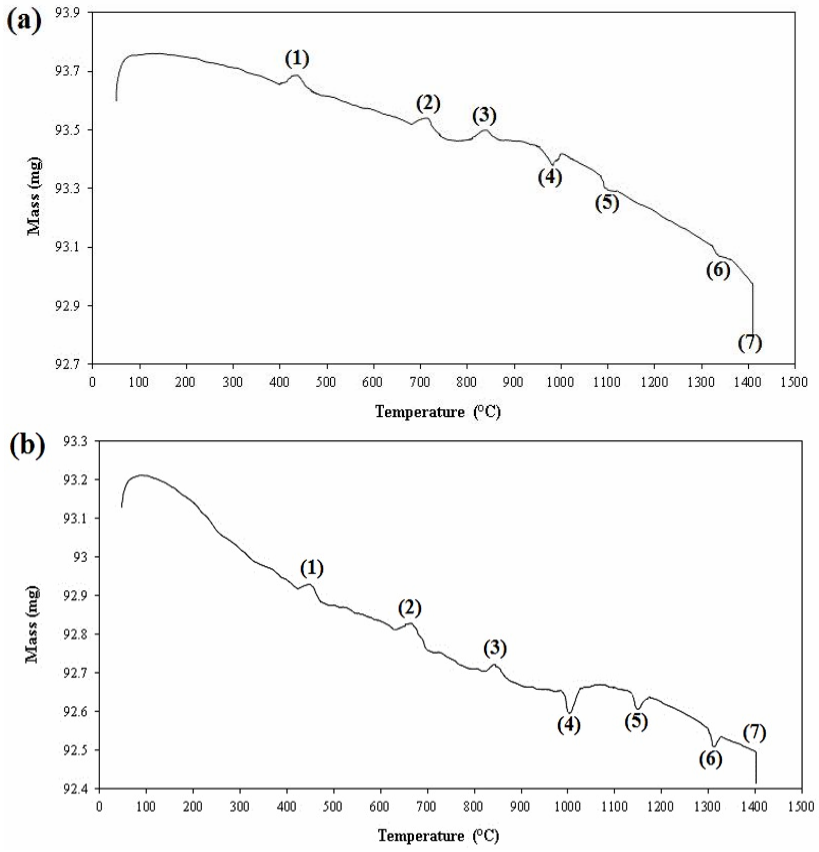

Fig. 3. Curve obtained from DTA test a) A286 and b) Nb-A286.

[DOI: 10.22068/ijmse.18.1.7]

To investigate the stability of γ' phase in A286 and Nb-A286 alloys, differential thermal analysis (DTA) was performed on the solution annealed samples. The DTA results for the A286 and Nb-A286 alloys in the heating cycle are presented in Fig. 3. According to Fig. 3, points 1, 2, and 3 show the formation temperatures of the regions of GP, γ' phase, and η phase, while points 4, 5, 6, and 7 represent the dissolution temperatures of the γ', η and MC phases and melting point, respectively [9]. Table 2 shows the temperatures corresponding to points 1 to 7 for the A286 and Nb-A286 alloys. As shown in table 2, the formation temperature of the γ' strengthening phase in A286 decreases from 705 to 687 °C for Nb-A286 alloy. Besides, the dissolution temperature of the γ' phase in A286 increases from 982 to 1007 °C for Nb-A286 alloy. Therefore, the addition of niobium to A286 superalloy increases the thermal stability of the γ' phase.

3.2. Simulation of Phase Formation via JMatPro Software

The γ' phase transformation to η phase was carefully investigated using JMatPro thermodynamic software. Figs. 4 and 5 show the simulated TTT and CCT diagrams for the A286 and Nb-A286 alloys. The critical temperatures extracted from these diagrams are presented in table 3.

As shown in table 3, on the one hand, the γ' phase in Nb-A286 superalloy is formed at a lower temperature and dissolved at a higher temperature than the A286 alloy, and on the other hand, the formation of the η phase also occurred at a higher temperature in Nb-A286 alloy. This indicates an increased stability of the γ' phase in the -A286 superalloy and a delay in η phase formation. These changes are in line with the results of the DTA test and are consistent with each other.

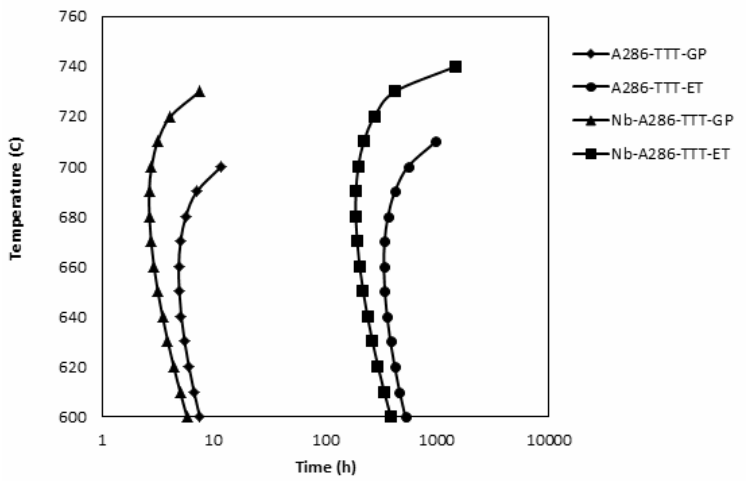

Fig. 4. TTT curve plotted by JMatPro software.

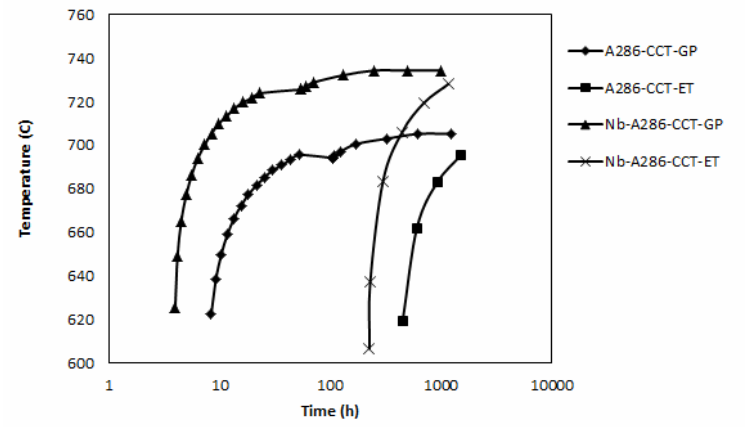

Fig. 5. CCT curve plotted by JMatPro software.

[DOI: 10.22068/ijmse.18.1.7]

Table 3. Critical temperatures extracted from simulated diagrams by JMatPro software for A286 and Nb-A286 superalloys.

Alloy \ Critical Temperature	$T_f\gamma'$	$T_f\eta$	$T_s\gamma'$	$T_s\eta$	T_{incip}	T_m
A286	618	625	1050	710	1060	1400
Nb-A286	600	680	1035	880	1045	1397

Comparing the diagrams in Fig. 5 shows that the γ' phase stability range in the Nb-A286 alloy is broader than the A286 alloy.

3.3. Evaluation of High-Temperature Tensile Properties

To investigate the tensile behavior of A286 and Nb-A286 superalloys at high temperatures, the tensile test was carried out at 650 °C, which is close to the service temperatures of this superalloy. Single-stage (720 °C for 16 h) and two-stage (720 °C for 16 h and 820 °C for 4 h) aging heat treatment were performed on both A286 and Nb-A286 alloys to investigate the simultaneous effects of the rate and morphology of the η phase as well as the effect of the niobium addition on the high-temperature tensile properties. Figs. 6 (a and b) show the tensile test diagrams for these alloys in two modes of single-stage and two-stage aging heat treatments. The results of the hot tensile tests (HTTs) are presented in table 4. It is worth noting that all the hot tensile diagrams are engineering curves.

According to Fig. 6 and the results of table 4, the addition of niobium to A286 superalloy improves the yield and ultimate tensile strength and increases the elongation of this alloy. The presence of the niobium element with a larger radius than the matrix causes a network strain in the austenite matrix and thereby increases the strength [29-31].

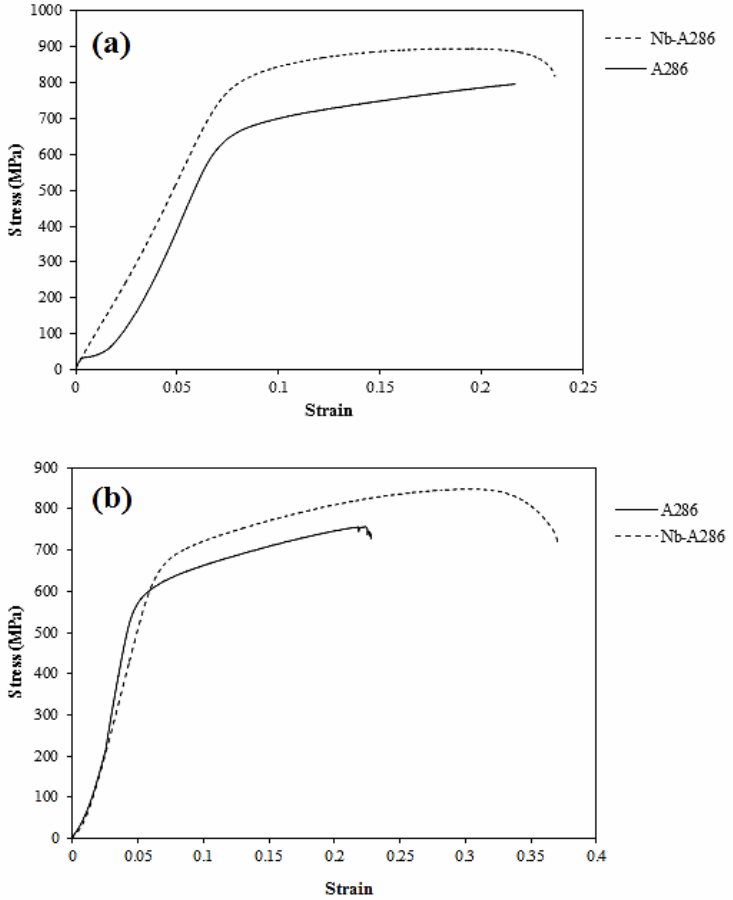

Fig. 6. a) Engineering curves of hot tensile test at 650 °C after single-stage aging at 720 °C for 16 h and b) Engineering curves of hot tensile test after two-stage aging at 720 °C for 16 h and 820 °C for 4 h.

[DOI: 10.22068/ijmse.18.1.7]

Table 4. Tensile properties of A286 and Nb-A286 superalloys after single-stage and two-stage aging heat treatment.

	Aging Temperature (°C)	Aging Time (h)	Yield Strength (MPa)	UTS (MPa)	Elongation (%)	η Volume Fraction (%)
A286	720	16	580	793	20.9	0
	820	8	554	749	22.3	3.5
Nb-A286	720	16	627	894	21.8	0
	820	8	650	849	36.7	1

By comparing the results of the tensile test after one-stage and two-stage aging, it can be concluded that the strength of the over-aged specimens is lower than the standard ones. Fig. 7 shows the SEM BSE mode image of the growth and dissolution of γ' precipitations. The formation of the η phase, the creation of γ' depleted zones between the η layers as a result of over-aging soften the matrix by eliminating the strengthening phase and reducing the specimens strength in the over-aging conditions. It should be noted that the needle morphology of the η phase in A286 alloy is also a factor in the loss of mechanical properties. In contrast, the alloy elongation in the over-aging state was significantly (about 14 %) higher than that of the standard sample. This increase can be attributed to the orientation of the η phase with the matrix and its deformation in the tensile direction. Fig. 8 shows an SEM image of the η phase elongation during the tensile test. The softening of the matrix due to the formation of γ' depleted zones as well as the η phase ability to deform with the matrix cause the alloy to increase flexibility. The presence of η phase with cellular morphology at the grain boundary can improve the strength [31, 32].

The fracture surfaces of the alloy after tensile testing are depicted in Fig. 9. The presented fracture surfaces show dimple-ductile fracture characteristics. The mechanism proposed by Ashby [30, 33] states that the cavities nucleate alongside secondary phase precipitations (γ' and η). It is suggested that the cavity was nucleated during the sliding/climbing of the dislocations, due to the precipitate pinning effect and the impeding grain boundary during grain boundary sliding. The component will be susceptible to fracture if the cavities sufficiently enlarge and joint together. Vacancies can agglomerate and form stable voids. The γ' and η precipitations are harder than the γ matrix, affecting both the elastic and plastic zones. The consequential dissonance results in the stress concentration alongside the precipitation. The created stress increases in the form of plastic strain. This process continues until the removal of the precipitation from the matrix. Then, a cavity is created and the sample breaks. In the A286 sample, the cavities are deeper than the Nb-A286 sample, indicating improved mechanical properties due to the addition of niobium.

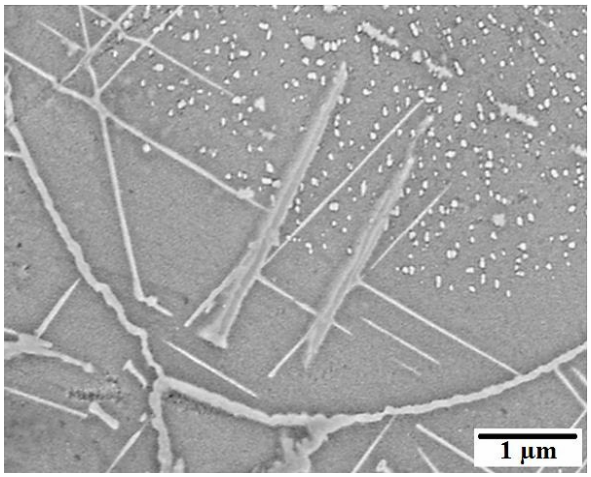

Fig. 7. SEM BSE mode image of γ' and η precipitations after two-stage heat treatment at 720 °C for 16 h and 820 °C for 4 h in the A286 sample.

[DOI: 10.22068/ijmse.18.1.7]

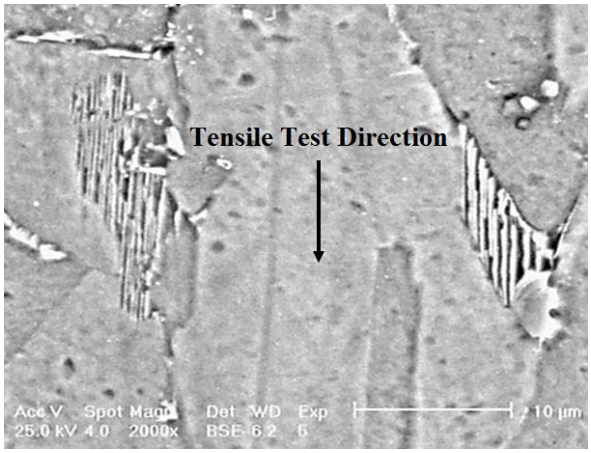

Fig. 8. The SEM image of the η phase elongation after the HTT in sample A286.

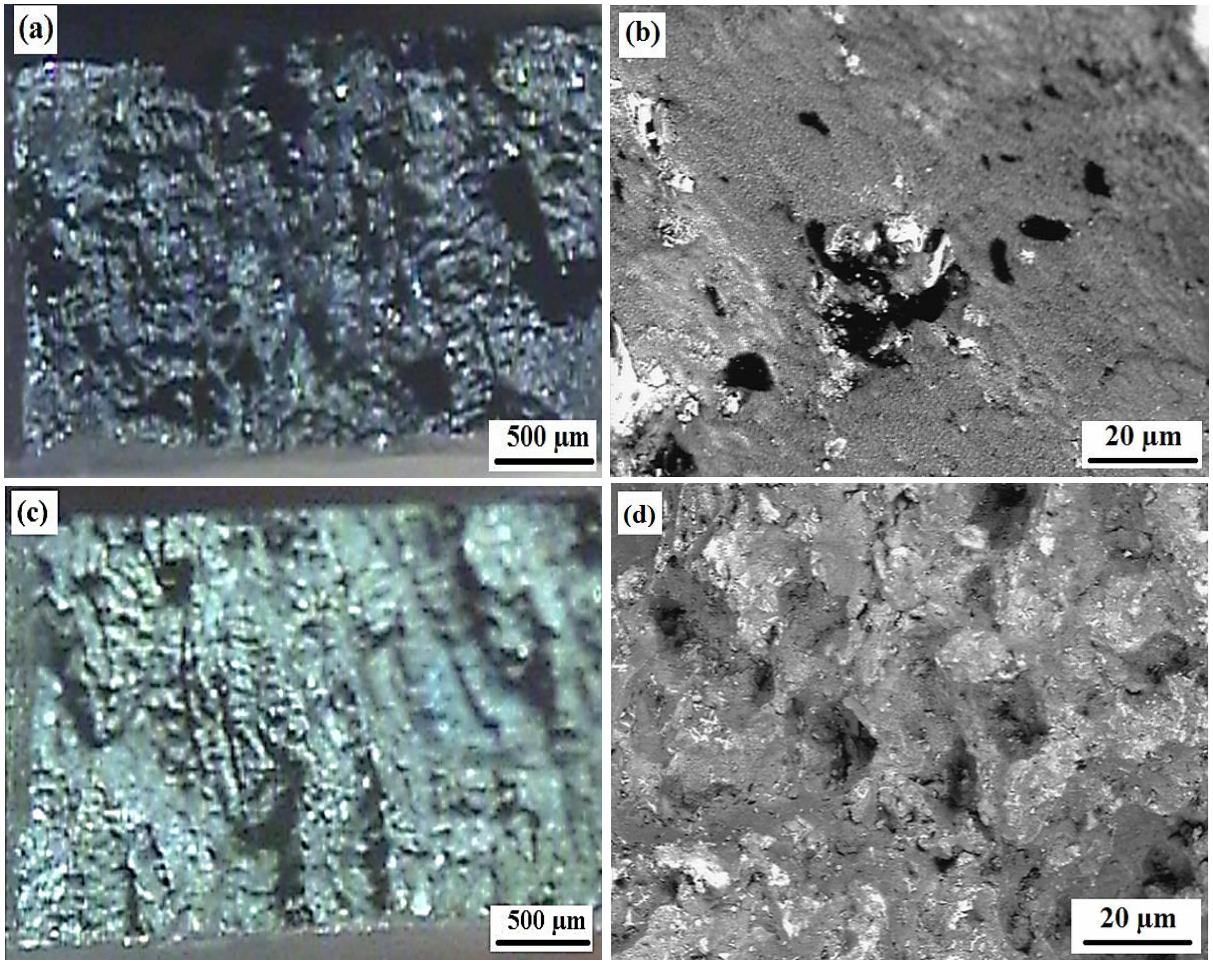

Fig. 9. Fracture surfaces of samples of a) and b) A286, c) and d) Nb-A286 aged at 820 °C for 4 h after the tensile test at 650 °C (the right images with higher magnification, present the center of the fracture surface of the left images).

4. CONCLUSION

Based on the results of the current study, the following results were obtained:

1- The hot tensile results showed that the addition of niobium increased both strength and elongation. This was due to an increase in the volume fraction of the γ' strengthening phase with more stability and prevention of the Widmanstatten η phase. Also, the increase in the strength of the γ matrix phase

[DOI: 10.22068/ijmse.18.1.7]

due to the dissolution of niobium in the matrix, and the creation of network strain in the matrix phase were other causes.

2- By comparing the results of the hot tensile tests after one-stage and two-stage aging, it was found that the over-aged specimens had lower strength and higher elongation (about 14 %) than standard specimens. The reason for the strength decrease is the growth and dissolution of γ' precipitations, the formation of η phase, the creation of γ' depleted zones between the η layers, and the formation of η phase with the Widmanstatten morphology. Also, the reason for the increase of the elongation was the softening of the matrix due to the formation of γ' depleted zones and the ability to deform the η phase within the matrix.

3- Based on the results of the DTA test and the simulated TTT and CCT diagrams for the A286 and Nb-A286 superalloys, it was found that the addition of niobium to A286 alloy reduced the formation temperature of γ' strengthening phase and increased the dissolution temperature of this phase. It also shifted the η phase formation to a higher temperature, resulting in a wider stability range of γ' phase in Nb-A286 alloy compared to the A286.

4- The results of the simulation with JMatPro software are consistent with the DTA test results and confirmed each other.

REFERENCES

1. H. De Cicco, M. I. Luppo, L. M. Gribaudo, J. Ovejero García, "Microstructural development and creep behavior in A286 superalloy", Mater Charact. A. 2004, 52, 85-92.
2. Z. Guo, H. Liang, M. Zhao, L. Rong, "Effect of boron addition on hydrogen embrittlement sensitivity in Fe-Ni based alloys", Mater Sci. Eng. A. 2010, 527, 6620-6625.
3. M. J. Zhao, Z. F. Guo, H. Liang, L. J. Rong, "Effect of boron on the microstructure, mechanical properties and hydrogen performance in a modified A286", Mater. Sci. Eng. A. 2010, 527, 5844-5851.
4. J. Nakamura, M. Miyahara, T. Omura, H. Semba, M. Wakita, "Fatigue Properties and Degradation Mechanism for Stainless and High Strength Steels in High Pressure Gaseous Hydrogen Environment", Zairyou. 2011, 60, 1123-1129.
5. P. Zhang, Q. Zhu, C. Hu, C. Wang, G. Chen, H. Qin, "Cyclic deformation behavior of a nickel-base superalloy under fatigue loading", Mater Des. 2015, 69, 12-21.
6. M. J. Zhao, Z. F. Guo, H. Liang, L. J. Rong, "Effect of boron on the microstructure, mechanical properties and hydrogen performance in a modified A286", Mater Sci. Eng. 2010, 527, 5844-5851.
7. M. Savoie, C. Esnouf, L. Fournier, D. Delafosse, "Influence of ageing heat treatment on alloy A-286 microstructure and stress corrosion cracking behavior in PWR primary water", J. Nucl. Mater. 2007, 360, 222-230.
8. N. Tajima, A. Orita, T. Matsuo, Y. Yamaguchi, J.Yamabe and S.Matsuoka, "Effect of Internal Hydrogen on Tensile Properties of Iron-Based Superalloy SUH 660", Transactions of the JSME. 2012, 78, 1173-1188.
9. M. Seifollahi, S. H. Razavi, S. H. Kheirandish, S.M. Abbasi, "The mechanism of h phase precipitation in A286 superalloy during heat treatment", J. Mater Eng. Perform. 2013, 22, 3063-3069.
10. J. C. Zhao, V. Ravikumar, A. M. Beltran, "Phase precipitation and phase stability in Nimonic 263", Metall. Mater Trans. A. 2001, 32, 1271-1283.
11. P. M. Mignanelli, N. G. Jones, M. C. Hardy, H.J. Stone, "The influence of Al:Nb ratio on the microstructure and mechanical response of quaternary Ni–Cr–Al–Nb alloys", Mater. Sci. Eng. A. 2014, 612, 179-186.
12. P. M. Mignanelli, N. G. Jones, M. C. Hardy, H. J. Stone, "On the Effect of Alloying Additions to the Ni-Cr-Al-Nb Dual-Superlattice Gamma-Gamma Prime-Gamma Double Prime Superalloys", Aerospace, and Industrial Applications, The Minerals, Metals & Materials Series. 2018, 679-690.
13. X. Xie, J. Dong, G. Wang, W. You, J. Du, C. Zhao, "The effect of Nb, Ti, Al on precipitation and strengthening behavior of 718 type superalloys", In: Loria E, editor. Superalloy 718, 625 and various derivatives, The Minerals, Metals and Materials Society. 2005, 287-298.

[DOI: 10.22068/ijmse.18.1.7]

14. J. P. Collier, S. H. Wong, J. C. Phillips, J. K. Tien, "The effect of varying Al, Ti, and Nb content on the phase stability of Inconel 718", Metal. Trans A. 1988, 19, 1657-1666.
15. B.S. Rho and S.W. Nam, "Fatigue-Induced Precipitates at Grain Boundary of Nb-A286 Alloy in High Temperature Low Cycle Fatigue", Mater. Sci. Eng. A. 2000, 291, 54-59.
16. B. S. Rho, S. W. Nam, X. Xie, "The effect of test temperature on the intergranular cracking of Nb-A286 alloy in low cycle fatigue", J. Mater Sci. 2002, 37, 203-209.
17. B. S. Rho, K. J. Kim, and S. W. Nam, "The Effect of Hold Time and Waveform on the High-Temperature, Low-Cycle Fatigue Properties of a Nb-A286 Alloy", Metallurgical and Materials Transaction A. 2001, 32, 2539-2546.
18. M. Seifollahi, S. H. Kheirandish, S. H. Razavi, S. M. Abbasi, P. Sahrapour, "Effect of η Phase on Mechanical Properties of the Iron-based Superalloy Using Shear Punch Testing", ISIJ International. 2013, 53, 311-316.
19. M. Seifollahi, P. Sahrapour, S. M. Abbasi, S. H. Kheirandish, S. H. Razavi, "Mathematical-Thermodynamic Prediction and Kinetics of Eta Phase Formation in Fe–Ni-Based Superalloys", Trans Indian Inst Met. 2018, 71, 147-152.
20. M. Seifollahi, S. H. Kheirandish, S. H. Razavi, S.M. Abbasi, "The precipitation of η phase in an Fe-Ni-based superalloy with different Ti/Al ratios", Int J Mater Res. 2013, 104, 344-350.
21. L. Kaufman, "Computer Calculation of Phase Diagrams", Academic Press. 1974, 5, 1617-1621.
22. L. Viskari, K. Stiller, "Atom probe tomography of Ni-base superalloys Allvac 718Plus and Alloy 718", Ultramicroscopy. 2011, 111, 652-658.
23. P. Sahrapour, M. Seifollahi, S. M. Abbasi, "Effect of Annealing Temperature on Punching Shear Strength of Nb-A286 Superalloy", Trans Indian Inst Met. 2018, 71, 1003-1010.
24. G. D. Smith and S. J. Patel, "The role of niobium in wrought precipitation-hardened nickel-base alloys", In: Loria E, editor. Superalloy 718, 625 and various derivatives, The Minerals, Metals and Materials Society. 2005, 135-154.
25. Z. Zhong, Y. Gu, Y. Yuan, "Microstructural stability and mechanical properties of a newly developed NieFe-base superalloy", Mater Sci. Eng. A. 2015, 622, 101-107.
26. Lopez-Galilea, J. Koßmann, A. Kostka, R. Drautz, L. Mujica Roncery, T. Hammerschmidt, S. Huth, W. Theisen, "The thermal stability of topologically close-packed phases in the single-crystal Ni-base superalloy ERBO/1", J Mat Sci. 2016, 51, 2653-2664.
27. B. Piekarski, "Effect of Nb and Ti additions on microstructure, and identification of precipitates in stabilized Ni-Cr cast austenitic steels", Materials Characterization. 2001, 47, 181-186.
28. L. Xudong, D. Jinhui, D. Qun, Z. Jingyun, "Stress rupture properties of GH4169 superalloy", Jmaterrest echol. 2014, 3, 107-113.
29. T. Zaman, M. Farooque, S. A. Rizvi, I. Salam, M. Waseem, "Investigation of low stress rupture properties in Inconel-718 super alloy", IOP Conference Series: Materials Science and Engineering. 2016, 146, 1-7.
30. Y. Zhi-hao , W. Shao-cong , D. Jian-xin , Y. Qiu-ying , Z. Mai-cang , H. Guang-wei , "Constitutive behavior and processing maps of low-expansion GH909 superalloy", International Journal of Minerals, Metallurgy and Materials. 2017, 24, 432-443.
31. X. Xishan, M. Zhengdong, D. Jianxin, H. Yaohe, "High Temperature Creep, Fatigue and Creep/Fatigue Interaction Behavior of γ' Strengthened Austenitic Iron-Base Superalloy", Trans Tech Publications. 2005, 297, 1458-1463.
32. S. Mannan, S. Patel, "A new Ni-base superalloy for oil and gas applications", TMS. 2008, 31-39.
33. M.F. Ashby, C. Gandhi, and D.M.R. Taplin, "Overview No. 3 fracture-mechanism maps and their construction for f.c.c. metals and alloys", Acta Metallurgica. 1979, 27, 699-729.

[DOI: 10.22068/ijmse.18.1.7]